# Diffusion and Flow Birefringence of Poly(naphthoyleneimide benzimidazole) in Concentrated Sulfuric Acid

**P. N. Lavrenko***

*Institute of Macromolecular Compounds, Russian Academy of Sciences, 199004 St.-Petersburg, Russia*

**N. V. Pogodina**

*Institute of Physics, St.-Petersburg State University, 199164 St.-Petersburg, Russia*

*Received January 28, 1998*

ABSTRACT: The effect of changes in chemical structure on the equilibrium and kinetic behavior is examined for fully cyclic poly(naphthoyleneimide benzimidazole) (PNI) molecules in dilute solution in 96% sulfuric acid. With this aim, hydrodynamic and dynamo-optical properties were analyzed over a wide range of molecular weight from $6.7 \times 10^3$ to $2.5 \times 10^5$. The $M$ dependence of the translational diffusion coefficient, $D$, the shear optical coefficient, $\Delta n/\Delta\tau$, the intrinsic orientation of the macromolecules in the flow, $[\chi/g]$, and the intrinsic viscosity, $[\eta]$, were established as well as the macromolecule conformation. Results thus obtained indicate the rigid-chain behavior of the PNI molecules. From their comparison with similar data obtained earlier for poly(amide benzimidazole) the conclusion was made that the exclusion of physical mechanisms of the chain flexibility due to the amide group leads to a significantly higher equilibrium rigidity of the macromolecule. At the same time, the comparison of the flow birefringence relaxation time with the viscometric data indicates the intramolecular motions that include a large-scale deformation of the PNI chain increasing with the molecular weight.

## Introduction

Researching the synthesis of new polyheteroarylenes has provided a wide field for the experimental treatment of the macromolecule conformation by methods of molecular hydrodynamics and dynamo-optics.[1−6] Investigation of poly(amide benzimidazole) (PABI) molecular properties has shown[3,4] that the conformation of the PABI molecules is determined by peculiarities of the repeat chain unit chemical structure, which are the cause of the macromolecule chain coiling in solution and may be classified as some kind of molecule flexibility mechanism. Three such mechanisms for the PABI chain may be distinguished.

The first and most significant one, *structural* mechanism, is connected with a chain bend at the benzimidazole ring position. This leads to a break of the contour chain direction by an angle close to 30°, disturbing the coaxial ("crank-shaft") conformation of the para-aromatic polyamide chain.[1,7] The second and third mechanisms are both connected with the presence of the amide groups in the polymer chain. The valency angles $\alpha$ and $\beta$ formed by bonds at C and N atoms in the amide group are different, the difference $\alpha - \beta$ being from 6 to 12°.[8] This additional chain bend provides a second *structural* mechanism. Finally, noncoplanarity of the amide group caused by thermal oscillations of the inner angles, leads to a third alteration in the contour chain direction by the angle $\varphi$ close to 14°.[7] This can be classified as the third, *deformational* mechanism of the PABI chain equilibrium flexibility.

Considerable experimental data have allowed Tsvetkov[7] to formulate the principle of the addition of flexibilities for the aromatic polyamide chain. Thus, the smaller set of flexibility mechanisms (available by changing the chain chemical structure) has to lead to a higher equilibrium rigidity of the macromolecule. In fact, when the first mechanism is excluded, the persistence length of the chain, which is the measure of the chain rigidity, increases 2−3 times. This was shown, e.g., for poly(*p*-phenyleneterephthalamide) (PPTA).[2,3] Similar observations may be also assumed for the other flexibility mechanisms.

To test a part of the second and third mechanisms of the chain flexibility named above, in the present work, a new polymer having no amide groups has been investigated. This is poly(naphthoyleneimide benzimidazole) (shortly PNI), i.e., the polymer based on the dianhydride of 1,4,5,8-naphthylenetetracarboxylic acid and 5-amino-2-(*p*-aminophenyl)benzimidazole[9] with a structure shown below.

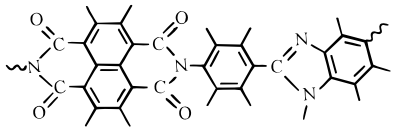

PNI looks like a better model for conformational investigations than other polyphthalimides because of the absence of so-called "defective" units (mainly, noncyclic), which disturb the regular semiladder structure of the chain.[10] The absence of such units is known to be the main requirement for success in the analysis of the heterocyclic polymer made by hydrodynamic and dynamo-optical methods. Note that many studies on the molecular characterization of the rigid-chain polyheteroarylenes concerning the degree of backbone coiling and some fundamental relationships, such as the intrinsic viscosity dependence on the molecular weight, were not well quantified because of different reasons.[11] It is often, first, that high molecular weight polymer samples are not available, and their quality is not sufficient to permit systematic studies. Second, these polymers are not usually soluble in organic solvent, but they are soluble in strong mineral acids such as a concentrated sulfuric one. This solvent is difficult to characterize, and its corrosive and hydroscopic nature

10.1021/ma980118o CCC: $15.00 © 1998 American Chemical Society
Published on Web 11/14/1998

requires special equipment. High solvent viscosity presents an additional difficulty for the careful purification of the polymer solution that is important when the light scattering technique is applied. Therefore, not so many successful applications of the last method are known.[11−15]

In the present work, the molecular properties of the PNI in concentrated sulfuric acid have been investigated by the methods of molecular hydrodynamics and dynamooptics: translational diffusion, flow birefringence (FB), and viscometry. The main aim was to characterize the degree of coiling and kinetic flexibility of the macromolecule in solutions and to compare the conformational parameters of the PNI and PABI macromolecules. Such a comparison is useful because the amide group of the PABI chain, −NH−CO− forms a part of the six-membered heterocycle in the PNI chain:

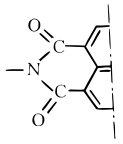

Therefore, we could evaluate the changes in conformation and equilibrium rigidity of the chain caused by this replacement of the amide bond to the heterocycle, which are undoubtedly responsible for the unique mechanical properties[16,17] and unusually high chemo- and thermostability of PNI.[18]

A low molecular weight compound with the structure shown below has been also investigated as a model suitable for the PNI repeat chain unit.

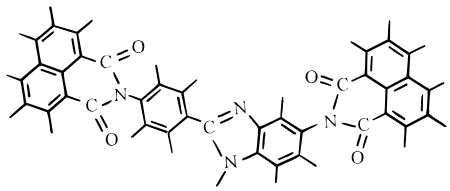

## Experimental Section

**Materials.** The PNI samples were prepared by high-temperature polycondensation varying the conditions of synthesis so as to obtain samples with different molecular weights.[9]

A particular lot of 96% sulfuric acid was used as a solvent with viscosity of $\eta_s^{30} = 0.1649$ g cm$^{-1}$ s$^{-1}$ and a density of 1.8255 g cm$^{-3}$ at 30 °C, and $\eta_s^{21} = 0.222$ g cm$^{-1}$ s$^{-1}$ and refractive index of $n_D = 1.4375$ at 21 °C. In this solvent, the polymer forms real solutions and does not undergo noticeable degradation. The solutions were prepared for 5−10 days with magnetic stirring at room temperature directly before measurements.

**Instruments and Experiments.** Translational diffusion was investigated at 30 °C with the DAK-4 diffusometer[19] of convectional type, in a Teflon cell 2.0 cm thick, as described previously.[3] The interferometric patterns were treated by the high-area method to determine the second central moment (dispersion) $\bar{\Delta}^2$ of the diffusion curve. Diffusion coefficient $D_T$ was then calculated as a slope of $\bar{\Delta}^2$, plotted against time $t$ by $\bar{\Delta}^2 = \text{const} + 2D_T t$. The diffusion curve area was used also to evaluate the refractive increment.[7]

The flow birefringence experiments were performed at 21 °C with a standard compensation photoelectric method applying the modulation of ellipticity of the polarized light.[20] The He−Ne laser with the wavelength 632.8 nm was used as a light source. A mica 0.04-wave plate was applied as a compensator. A Teflon dynamo-optimeter with an inner rotor of 3.0 cm length and with a gap of 0.02 cm was used. The flow birefringence effect in the solvent was negligible.

The solution viscosity was measured at 30 °C with an Ostwald type viscometer at an average flow shear rate of 106 s$^{-1}$. The intrinsic viscosity, $[\eta]$, was calculated in the usual way from the $c$ dependence of the inherent viscosity. The Huggins constant was found to be $k_H = 0.50 \pm 0.07$ as the average of the 23 samples tested.

The experimental data were treated with a least mean-square fit, the points scattered being characterized by the linear (power) correlation coefficient, $r$.

**Table 1. Hydrodynamic Properties of the PNI Samples[a]**

| $M_{D\eta}$ (×10$^{-3}$) | $[\eta]$ (×10$^{-2}$) (mL/g) | $D$ (×10$^{7}$)[b] (cm$^2$/s) | $(\Delta n/\Delta c)_{546}$[b] (mL/g) |
|---|---|---|---|
| 252 | 12.6 | 0.045 | 0.26 |
| 238 | 11.0 | 0.048 | 0.24 |
| 194 | 10.2 | 0.052 | 0.29 |
| 158 | 11.8 | 0.053 | 0.24 |
| 154 | 10.8 | 0.055 | 0.27 |
| 126 | 8.0 | 0.065 | |
| 105 | 7.4 | 0.071 | 0.26 |
| 86 | 5.1 | 0.086 | 0.23 |
| 65 | 4.25 | 0.100 | |
| 61 | 3.8 | 0.106 | 0.25 |
| 55 | 5.2 | 0.099 | 0.18 |
| 52 | 4.9 | 0.103 | 0.25 |
| 52 | 4.0 | 0.110 | 0.20 |
| 52 | 3.8 | 0.112 | 0.22 |
| 38 | 4.0 | 0.122 | 0.23 |
| 37 | 4.0 | 0.123 | 0.23 |
| 35 | 3.6 | 0.130 | 0.26 |
| 31 | 2.18 | 0.160 | 0.26 |
| 28 | 1.95 | 0.172 | 0.24 |
| 14 | 1.26 | 0.250 | 0.29 |
| 14 | 1.04 | 0.270 | 0.25 |
| 13.5 | 0.89 | 0.285 | 0.25 |
| 6.7 | 0.52 | 0.43 | 0.26 |
| 0.58467[c] | 0.047 | 1.80 | 0.24 |

[a] 96% $H_2SO_4$, 30 °C. [b] Each result is the average over two or three realizations with same conditions. [c] Formula weight for model compound $C_{12}H_6NO_2-C_7H_4N_2-C_6H_4-C_{12}H_6NO_2$.

## Results and Discussion

**Solution Properties.** Optical properties of PNI were used, first of all, to check the molecular dispersity of the polymer solution. With this aim in mind, the refractive index increment, $\Delta n/\Delta c$, was evaluated for polymer samples in solution at 546 nm. Results are collected in Table 1. One can see that these values found for different samples only slightly scatter about the averaged value $(\Delta n/\Delta c)_{546} = 0.24 \pm 0.02$ mL/g obtained over 21 test samples. Hence, there are no noticeable differences in solubility and optical homogeneity of the polymer samples with different molecular weights. The average value of $\Delta n/\Delta c$ obtained for PNI (0.24 mL/g) is somewhat smaller than that obtained earlier for PABI (0.29 mL/g)[3], which may be due to the different chemical structure of the polymers.

The solution viscosity was studied with several viscometers with different shear rates $g$, from 4 to 106 s$^{-1}$. It was shown that intrinsic viscosity is not affected by the gradient dependence over the shear rate range investigated.[10] The temperature coefficient of $[\eta]$ was determined for the sample with $M = 1.58 \times 10^5$ to be negative and equal $\Delta \ln[\eta]/\Delta T = -0.0046$ K$^{-1}$. This value is close to those found for other heterocyclic rigid-chain polymers, e.g., for PABI in 100% $H_2SO_4$ (−0.0045 K$^{-1}$)[21], and for "BBB" polymer in methanesulfonic acid (−0.0025 K$^{-1}$ ).[22]

Diffusion experiments were conducted with the linear dependence of the diffusion boundary dispersion $\bar{\Delta}^2$ on

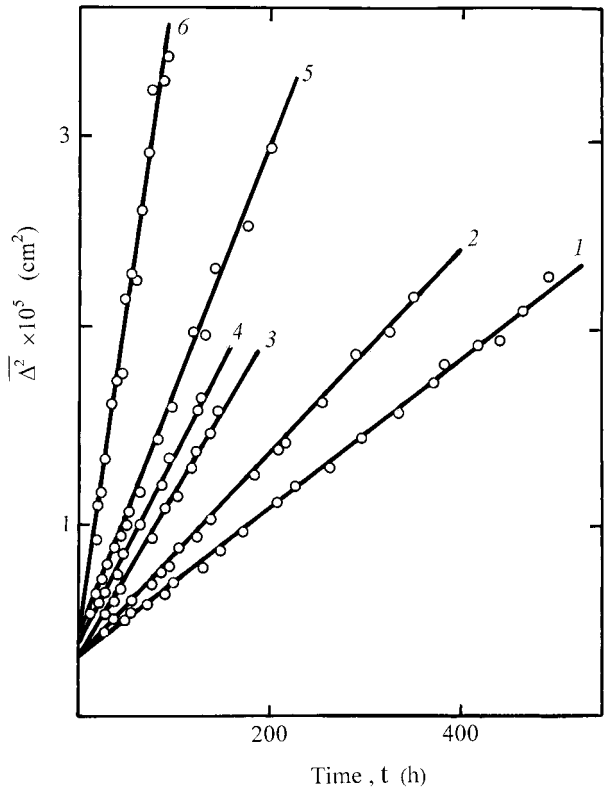


**Figure 1.** Typical results for dispersion of the diffusion curve $\bar{\Delta}^2$ vs time for PNI dissolved in 96% $H_2SO_4$ at 30 °C: $M_{D\eta} \times 10^{-3}$ = (1) 194, (2) 105, (3) 52, (4) 35, (5) 28, and (6) 6.7.

time (Figure 1) throughout the experiment, without decreasing the slope with time coursed by sample heterogeneity. This shows that the heterogeneity of the PNI samples is not significant, in accord with the PNI affiliation to a class of condensation polymers with the typical $M_w/M_n \leq 2$ values. For instance, the $M_z/M_w \leq 1.2$ values were obtained earlier for the PABI samples from the analytical ultracentrifugation data available in organic solvent.[3] The concentration dependence of the diffusion coefficient was negligible at the concentration used, $c \leq 0.1$ g/dL.

**Molecular Weight.** A direct measurement of molecular weight, $M$, is hindered here by the polymer insolubility in organic solvents. Therefore, $M$ was determined from diffusion−viscometric data by[23]

$$M_{D\eta} = (\Phi/P^3)[f]^3/[\eta] \quad (1)$$

on the assumption that the product $\Phi/P^3$ is independent of $M$ for the samples studied. Here $[f] \equiv f/\eta_s = k_B T/D_T \eta_s$, $f$ is the translational friction coefficient, $k_B$ is Bolzmann's constant, $T$ is the Kelvin temperature, and $P$ and $\Phi$ are defined as usual by the expressions

$$[f] = P\langle h^2\rangle^{1/2} \quad (2)$$

$$[\eta]M_L = \Phi\langle h^2\rangle^{3/2}/L \quad (3)$$

where $\langle h^2\rangle$ is the mean-square end-to-end distance, $M_L$ is the mass per unit length along the chain contour, $M_L = M/L$, and $L$ is the contour length of the macromolecule. In the coil limit ($L \to \infty$) when $P \to P_\infty \equiv \lim P_{L/A\to\infty}$ and $\Phi \to \Phi_\infty \equiv \lim \Phi_{L/A\to\infty}$, we may write $\langle h^2\rangle = AL$, where $A$ is the Kuhn statistical segment length, which is a measure of chain coiling (equilibrium flexibility).

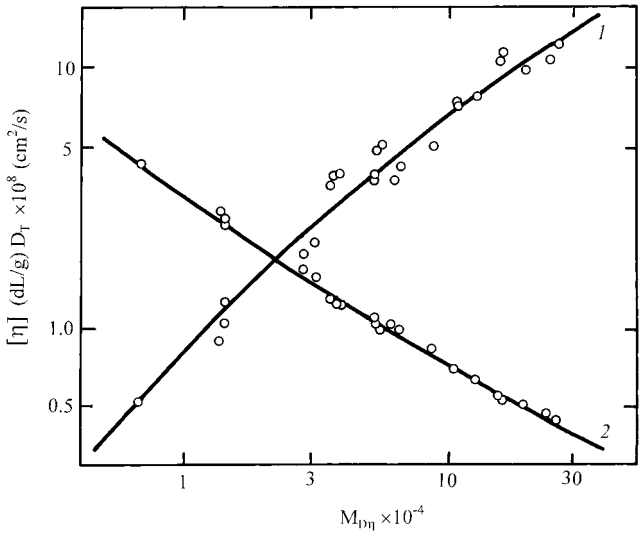


**Figure 2.** log−log plot of (1) $[\eta]$ and (2) $D_T$ vs $M_{D\eta}$ for PNI in 96% $H_2SO_4$. Solid curves represent the fit of the Yamakawa and Fujii treatment[28,29] for wormlike chains with $M_L = 25$ Da/Å, $A = 170$ Å, and $d = 8$ Å.

This method was recently analyzed in detail[23] in terms of the hydrodynamic invariant $A_0$ defined by[24]

$$A_0 = k_B P^{-1}(\Phi/100)^{1/3} \quad (4)$$

From this analysis we see that $\Phi/P^3$ (or $A_0$) is practically the $M$-independent product over the wide $M$ range. We use here $A_0 = 3.55 \times 10^{-10}$ erg deg$^{-1}$ mol$^{-1/3}$ as the value determined for PABI by the absolute (*sD*) method from the experimental hydrodynamic data.[3] This choice was confirmed by the experimental properties of the individual compound studied in the same solvent (last line in Table 1) as well as by the numerical $A_0$ value obtained as an average over all the experimental data available for rigid-chain polymers[23] to be $A_0 = (3.7 \pm 0.4) \times 10^{-10}$ erg deg$^{-1}$ mol$^{-1/3}$.

Hydrodynamic data are listed in Table 1. One can see exceptionally high $M$ values (up to $2.5 \times 10^5$), which were found for a rigid-chain fully cyclic polymer for the first time. Over a wide range of $M$, from $6.7 \times 10^3$ to $2.5 \times 10^5$, the $M$ dependence of $[\eta]$ and $D$ were then analyzed by using well-known empirical Kuhn−Mark expressions

$$[\eta] = K_\eta M^a \quad (5)$$

$$D = K_D M^{-b} \quad (6)$$

With $M$-independent numerical coefficients $K_\eta$, $K_D$, $a$ and $b$, the log−log plot of $[\eta]$ and $D$ against $M$ must be clearly a linear function. However, the data obtained for PNI (points in Figure 2) are not linear over all the $M$ range investigated. Therefore, they were approximated by curves with the slope decreasing with increasing $M$ (particularly, exponent $a$ from 1.20 to 0.60 and $b$ from 0.73 to 0.53).

**Macromolecule Dimensions from Diffusion and Viscometry Data.** High $a$ and $b$ values and their decrease with increasing $M$ are known to be typical for rigid-chain polymer with the extended conformation of the macromolecules.[25,26] This extended polymer chain is penetrable for the solvent flow, and this draining effect is decreasing with the increasing chain length along with increasing chain coiling. On the other hand,

the excluded volume effects are usually insignificant in a solution of rigid-chain polymer due to the weakened long-range interactions in the chain and may be often ignored.[7] The $[\eta](M)$ and $D(M)$ dependence as well as the dynamo-optical data discussed below, and a negative sign of $\Delta \ln[\eta]/\Delta T$, indicate the rigid-chain behavior of the PNI molecules in solution. Therefore, hydrodynamic theories[27−29] developed for wormlike chains, and taking into account the draining effects, were used to evaluate the degree of the chain coiling.

The following treatment of the diffusion and viscometric data was devised to determine the comformational parameters of the macromolecule. The coil limit behavior of a wormlike chain with length $L$, diameter $d$, and persistence length $a$ (Kuhn length $A = 2a$), according to the Hearst−Stockmayer theory,[27] may be described by

$$DM\eta_s/k_BT = P_\infty^{-1}(M_L/A)^{1/2}M^{1/2} + (M_L/3\pi)[\ln(A/d) - \gamma] \quad (7)$$

It is valid at $L/A \geq 2.28$ with $\gamma = 1.43$[27] or 1.056.[28] Hence, in the $L$ range indicated, the draining effects are not noticeable, and product $DM$ is predicted to be a linear function of $M^{1/2}$. In fact, many experimental $DM$ data plotted against $M^{1/2}$ follow a straight line.[7] This enables the simplest two-parameter description (and linear fit) of the experimental data.

Let us analyze eq 7 over the wide range of the molecular weight. The preceding expressions (2) and (3) may be combined with (7) to obtain the result

$$[f]^2/[\eta]M_L = c_1 + c_2([f]^3/[\eta]M_L)^{1/2} \quad (8)$$

with

$$c_1 = (P^3/3\pi\Phi)[\ln(A/d) - \gamma]$$

$$c_2 = (P^3/\Phi A)^{1/2}/P_\infty$$

Figure 3 shows $[f]^2/[\eta]M_L$ plotted against $([f]^3/[\eta]M_L)^{1/2}$, as calculated in frames of the theories[28,29] with theoretical $P$ and $\Phi$ values predicted for wormlike chains with different reduced length $L/A$ and diameter $d/A$. One can see the linear character of eq 8 (at least, within the error limits usual for the experimental data) predicted over all the range satisfying the condition $L/A \geq 2.28$. In other words, $c_1$ and $c_2$ do not practically depend here on the chain length, and the ratio $P^3/\Phi$ may be assumed equal to the Gaussian limit value $P_\infty^3/\Phi_\infty$. This permits us to use plot of (8), or an equivalent plotting of $(D^2[\eta])^{-1}$ against $(D^3[\eta])^{-1/2}$, to evaluate the conformational parameters of the macromolecule.

Figure 4 shows the experimental data obtained for PNI as $(D^2[\eta])^{-1}$ plotted against $(D^3[\eta])^{-1/2}$. This dependence was well approximated by the linear function

$$(D^2[\eta])^{-1} = K_1(D^3[\eta])^{-1/2} + K_2 \quad (9)$$

with

$$K_1 = (3.68 \pm 0.12) \times 10^2$$

$$K_2 = (4.65 \pm 0.66) \times 10^{12} \qquad (r = 0.9872) \quad (10)$$

in CGSE units. According to eq 7, the slope, $K_1$, is determined by $M_L/A$

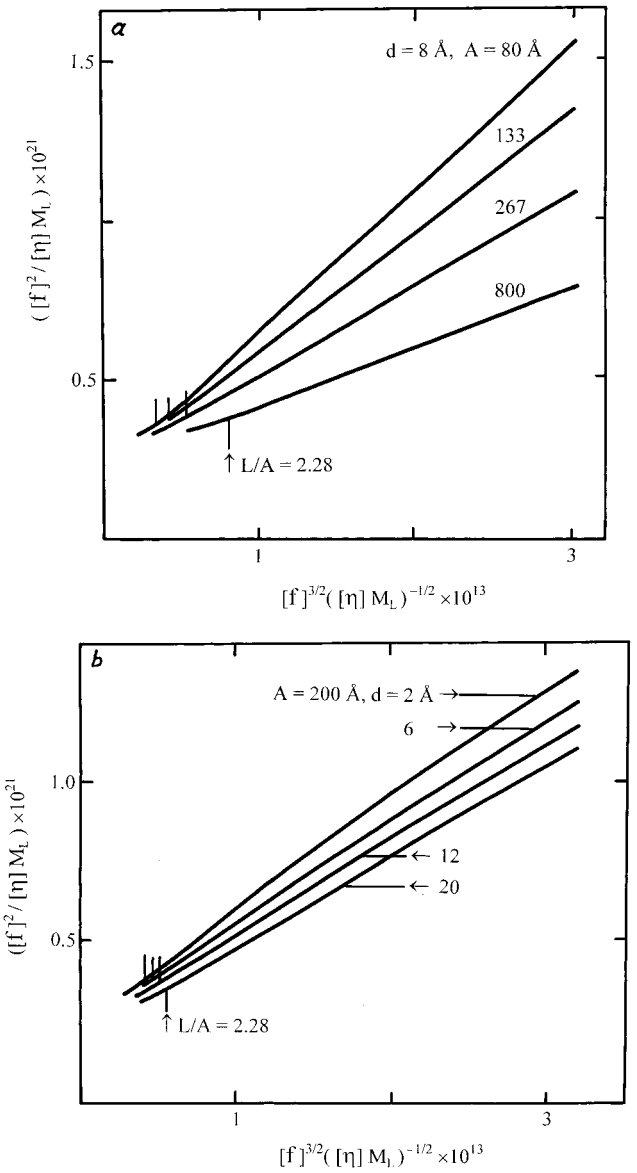


**Figure 3.** $[f]^2/[\eta]M_L$ vs $[f]^{3/2}([\eta]M_L)^{-1/2}$ calculated by eq 8 for wormlike model chains[28,29] with indicated values of $A$ from 80 to 800 Å (curves a) and $d$ from 2 to 20 Å (curves b).

$$K_1 = (k_B/10P_\infty)(\eta_s/A_0{}^3T)^{1/2}(M_L/A)^{1/2} \quad (11)$$

and the intercept, $K_2$, depends on the draining effect, i.e., on $A/d$

$$K_2 = (k_B/300\pi)(M_L\eta_s{}^2/A_0{}^3T^2)[\ln(A/d) - 1.056] \quad (12)$$

Using eqs 11 and 12 with $M_L = 25$ Da/Å (based on structure), $P_\infty = 5.11$,[28] $A_0 = 3.55 \times 10^{-10}$ erg deg$^{-1}$ mol$^{-1/3}$, and the result 10, we obtain a Kuhn length $A_D = 170 \pm 20$ Å (a persistence length of $85 \pm 10$ Å) and a chain diameter $d = 8 \pm 3$ Å.

Similar treatment of the hydrodynamic data by Vitovskaya et al.[3] obtained for PABI in $H_2SO_4$ leads to lower value, $A_{PABI} = 130 \pm 20$ Å. Hence, exclusion of the physical mechanisms of the chain flexibility connected with the amide groups (inequality of valence angles at C and N atoms in the amide group and its noncoplanarity) on passing from PABI to PNI leads to the increase in equilibrium rigidity of the chain from $A_{PABI} = 130$ to $A_D = 170$ Å. In other words, hydrodynamic properties confirm the assumptions made above.

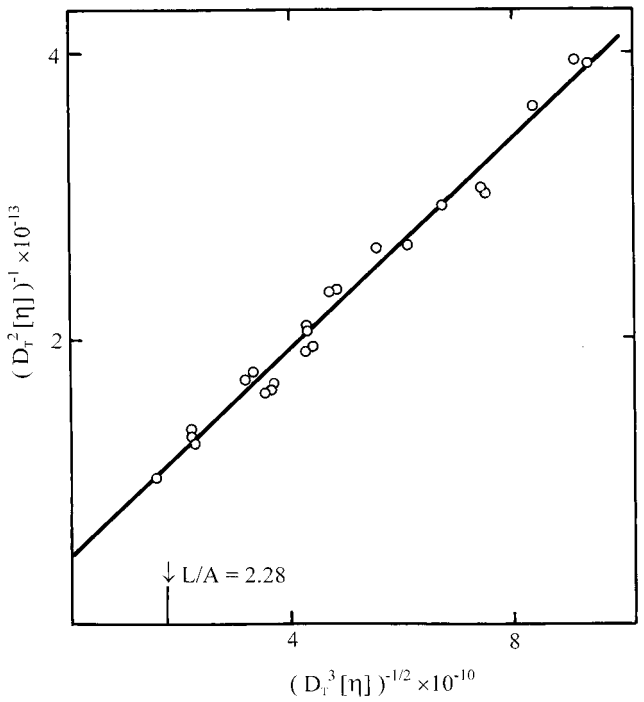


**Figure 4.** $(D_T^2[\eta])^{-1}$ vs $(D_T^3[\eta])^{-1/2}$ for PNI in 96% $H_2SO_4$ with $D_T$ and $[\eta]$ in $cm^2/s$ and $cm^3/g$, respectively (points). The solid curve presents a linear least mean-squares fit of all the experimental points satisfying the condition $L/A \geq 2.28$.

Polymolecularity effects were estimated in the usual way.[30] Inhomogeneity of samples may be taken into account during the calculation of the conformational parameters if we use, for instance, the parameters $\Phi^* = \Phi q_\eta$ and $P^* = Pq_f$ instead of $\Phi$ and $P$ in eqs 2 and 3. Polymolecularity correction factors, $q_\eta$ and $q_f$, were evaluated for PNI from Tables 8.1 and 9.1 given in ref 31 to be 0.955 and 1.022, respectively, with an assumed value 1.5 for $M_w/M_n$. This correction leads to a 5% fall in the $A$ value that, however, lies in limits of the experimental errors and cannot explain the difference between $A_{PABI}$ and $A_{PNI}$.

***M* Dependences of [η] and *D*.** As mentioned above, the dependences of $[\eta]$ and $D$ on $M$ in logarithmic scale (points in Figure 2) show the curvature decreasing with increasing $M$ in quantitative agreement with the predictions of the hydrodynamic theories (solid curves). The scaling exponents $a$ and $b$ in eqs 5 and 6 decrease monotonically with increasing $M$ (decreasing macromolecule drain). Hence, the Kuhn−Mark equation with constant numerical coefficients describes the molecular PNI properties in $H_2SO_4$ over a narrow $M$ range only.

Therefore, the other analytical presentation[26] based on the linearity of eq 8 was applied to describe the dependences under discussion over a broad $M$ range. Substituting $f$ in eq 8 with $M$, $[\eta]$, and $A_0$ according to eqs 2 and 4, we have

$$[\eta] = M^2(K_3 + K_4M^{1/2})^{-3} \tag{13}$$

where coefficients $K_3$ and $K_4$ are defined by

$$K_3 = 100^{2/3}(A_0T/\eta_s)^2K_2$$
$$K_4 = 10^{1/3}(A_0T/\eta_s)^{1/2}K_1 \tag{14}$$

Applying results of (10), instead of eq 13, we have

$$[\eta]\ (\text{mL/g}) = M^2[(42.6 \pm 6.0) + (0.64 \pm 0.02) \times M^{1/2}]^{-3} \tag{15}$$

Similarly, a transforming of eq 8 in relation to $[\eta]$ leads to the expression

$$D = M^{-1}(K_5 + K_6M^{1/2}) \tag{16}$$

with coefficients $K_5$ and $K_6$ defined by

$$K_5 = 100(A_0T/\eta_s)^3K_2$$
$$K_6 = 10(A_0T/\eta_s)^{3/2}K_1 \tag{17}$$

Using results of (10) in both (17) and (16), we have

$$D\ (\text{cm}^2/\text{s}) = M^{-1}[(1.29 \pm 0.18) \times 10^{-4} + (1.94 \pm 0.06) \times 10^{-6}M^{1/2}] \tag{18}$$

Equations 15 and 18 are valid over all the $M$ range investigated. In other words, the fact the numerical coefficients in eqs 13 and 16 are not as sensitive to change in $M$ as those in the Kuhn−Mark equations shows the wider applicability of eqs 13 and 16 to the analytical description of the PNI solution properties as a function of $M$. On the other hand, the two-parametric expressions 13 and 16 seem to be more convenient in practice than some other recent equations.[11]

**Intrinsic Orientation in FB.** The orientation (extinction) angle, $\varphi_m$, formed by the optical axis of solution and flow direction is the angle of preferable orientation of the macromolecule principal axis in the flow field. It is determined by the rotational mobility of the macromolecule and, hence, is also an important molecular characteristic. Particular attention was paid, therefore, to high precision measurements of $\varphi_m$. With the highly sensitive techniques applied, it was possible for PNI samples with $[\eta] \geq 0.65$ dL/g. Important to note that the dependence of $\varphi_m$ on the flow shear rate $g$ was observed with the start point at 45°. This is an obvious experimental proof that intermolecular association is negligible in a solution of all samples investigated.[7]

The linear part of the $g$-dependence of the orientation angle $\chi$, defined by $\chi = (\pi/4) - \varphi_m$, was sufficiently large for the reliable determination of the initial slope, $(\chi/g)_{g\to0}$ (Figure 5). This ratio was then extrapolated to zero concentration (Figure 6) to obtain the intrinsic orientation, $[\chi/g]$ as

$$[\chi/g] = \lim(\chi/g)_{g\to0,c\to0}$$

Experimental values of $[\chi/g]$ are listed in Table 2 and plotted in Figure 7 against $M$. The best power of $M$ in the least squares yields the scaling relation

$$[\chi/g]\ (\text{rad s}) = 1.53 \times 10^{-11}M^{1.44} \qquad (r = 0.9976) \tag{19}$$

which reflects the growth of the rotation friction coefficient with increasing $M$. Intrinsic viscosity is determined also by rotational mobility of the macromolecule in solution. Therefore, $[\chi/g]$ may be related to $[\eta]$ and $M$ by[7]

$$[\chi/g] = GM[\eta]\eta_s/RT \tag{20}$$

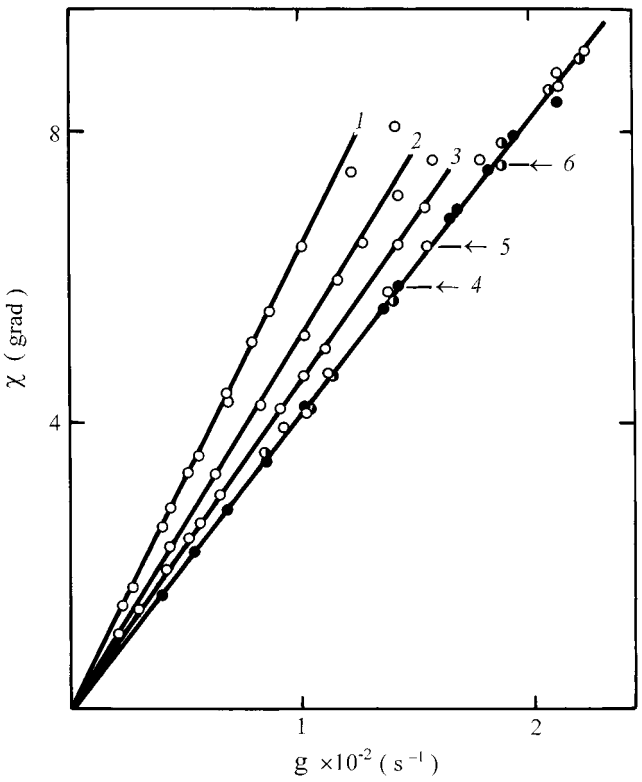


**Figure 5.** Orientation angle $\chi$ vs shear rate $g$ for a PNI sample with $M_\eta = 2.1 \times 10^5$ in solution in $H_2SO_4$ with solute concentration $c \times 10^4 =$ (1) 2.11, (2) 1.35, (3) 0.75, (4) 0.37, (5) 0.27, and (6) 0.20 g/mL.

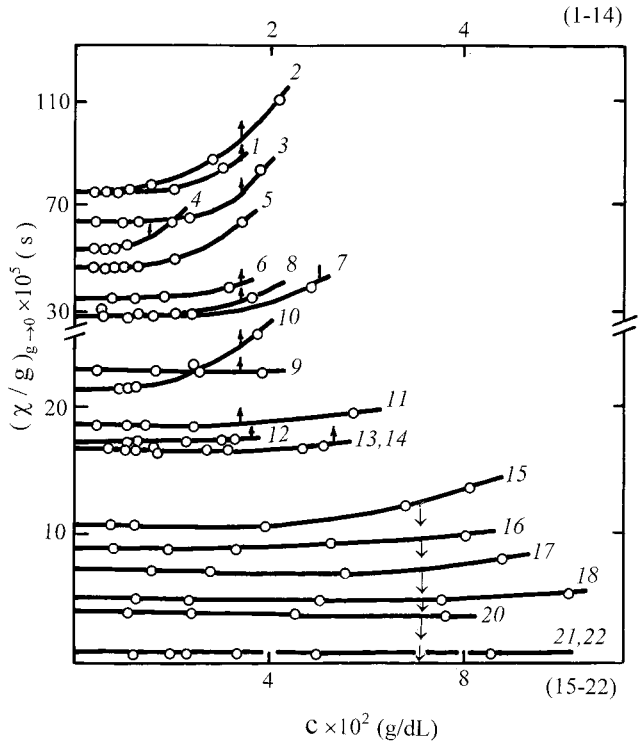


**Figure 6.** Concentration dependence of the orientation angle initial slope $(\chi/g)_{g\to 0}$. Numbers on the curves from 1 to 22 correspond to $M_\eta$ from $2.2 \times 10^5$ to $8.5 \times 10^3$ for PNI samples as they are listed in Table 2.

The numerical value of the model parameter $G$ is known to reflect the character of the polymer chain motion in the shear flow field. Figure 7 shows that the experimental $G$ value decreases with increasing $M$. For the first nine samples (low $M$) $G$ correlates with the theoretical value predicted for kinetically rigid chains, from 0.50 to 0.67.[33] The further decrease in $G$ with increasing $M$ indicates kinetic flexibility[7] of the PNI chain (deformational motion).

In other terms, Brownian rotational mobility of the particles always counteracts their kinematic orientation, which arises in the flow field. Therefore, the $[\chi/g]$ value, being independent of the particle optical properties, is simply related to the rotational diffusion coefficient, $D_r$, when a particle is rotating about its short axis, by

$$[\chi/g] = 1/(12D_r) \tag{21}$$

$D_r$ may be then expressed in the form[34]

$$N_A k_B T/D_r \eta_s = 4M[\eta]H \tag{22}$$

with

**Table 2. Dynamo-Optical Properties of the PNI Samples[a]**

| $[\eta]$ (×10 $^{-2}$) (mL/g) | $(\Delta n/\Delta\tau)$ (×10$^{10}$) (cm s$^2$/g) | $[\chi/g]$ (×10 $^5$) (s) | $G$ | $M_\eta$ (×10$^{-3}$)[b] |
|---|---|---|---|---|
| 12.0 | 441 | 77 | 0.33 | 220 |
| 11.7 | 436 | 76 | 0.35 | 210 |
| 11.2 | 435 | 66 | 0.33 | 200 |
| 10.4 | 428 | 55 | 0.33 | 180 |
| 9.35 | 433 | 48 | 0.37 | 155 |
| 8.4 | 428 | 35 | 0.35 | 133 |
| 8.0 | 430 | 30 | 0.34 | 125 |
| 7.7 | 420 | 29 | 0.36 | 117 |
| 7.2 | 414 | 23 | 0.33 | 108 |
| 7.0 | 422 | 22 | 0.34 | 103 |
| 5.5 | 405 | 17.0 | 0.46 | 75 |
| 5.5 | 399 | 17.0 | 0.46 | 75 |
| 4.5 | 388 | 10.8 | 0.46 | 59 |
| 3.9 | 391 | 9.0 | 0.52 | 50 |
| 3.3 | 376 | 7.5 | 0.62 | 41 |
| 2.7 | 366 | 5.1 | 0.64 | 33 |
| 2.5 | 371 | 4.6 | 0.69 | 30 |
| 2.4 | 376 | 4.1 | 0.68 | 28 |
| 0.70 | 285 | 0.66 | 1.23 | 8.6 |
| 0.68 | 285 | 0.63 | 1.22 | 8.5 |
| 0.63 | 340 | | | 7.9[d] |
| 0.32 | 200 | | | 4.5[d] |
| 0.30 | 260 | | | 4.2 |
| 0.10 | 110 | | | 1.9[d] |
| 0.047 | 40 | | | 0.58467[c] |

[a] 96% $H_2SO_4$, 21 °C. [b] Values calculated by eq 15. [c] Formula weight for model compound $C_{12}H_6NO_2{-}C_7H_4N_2{-}C_6H_4{-}C_{12}H_6NO_2$. [d] Samples obtained by the thermal hydrolysis of the PNI sample in solution as described previously.[32]

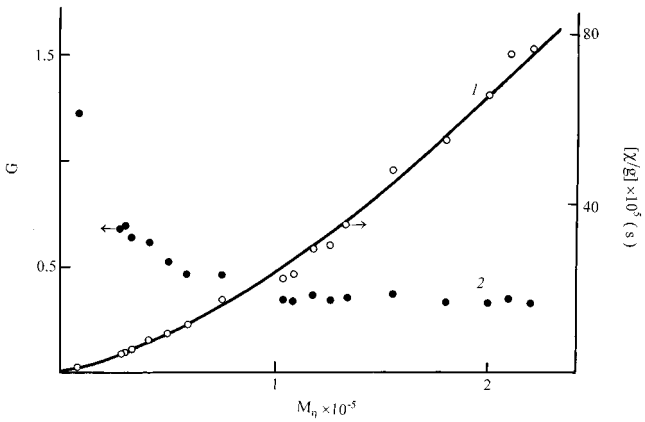


**Figure 7.** Intrinsic orientation $[\chi/g]$ (curve 1) and parameter $G$ vs molecular weight for PNI in 96% $H_2SO_4$ (points). The solid curve represents a fit of experimental data to eq 19.

$$H = \{1 + (0.64/2.88N_A)(\langle h^2\rangle^{1/2}/L)[\ln(A/d) - 1.43]\}^{-1} \quad (23)$$

According to this theory, for rigid wormlike chains rotating as a whole in frozen conformation, we have

$$\eta_s D_r M^2/k_B T = 0.72(M_L/A)^{3/2}M^{1/2} + 0.64(M_L{}^2/A)[\ln(A/d) - 1.43] \quad (24)$$

Hence, for the kinetically rigid penetrable macromolecules, the product $D_rM^2$ must be a linear function of $M^{1/2}$ with the slope determined by $(M_L/A)^{3/2}$ and with the intercept depending on the draining effect, i.e., on $A/d$.

Figure 8 represents the plot (24) for PNI. The slope of the tangent curve enables one to estimate a Kuhn length $A_r = 160$ Å, which is close to that obtained above from the hydrodynamic data ($A_D = 170$ Å). Deviation of the experimental points upward of the straight line at high $M$ indicates that the PNI molecules rotate in the flow field not as a whole but with intramolecular deformations increasing with increasing $M$.

**Flow Birefringence.** The shear optical coefficient, $\Delta n/\Delta\tau$, was determined from extrapolation of $\Delta n/gc\eta_s$ to vanishing concentration

$$\Delta n/\Delta\tau = \lim(\Delta n/gc\eta_s)_{g\to 0,c\to 0}$$

with $\Delta n$ being the birefringence observed in polymer solution with the solute concentration $c$ at the shear rate $g$. Strong dependence of $\Delta n/\Delta\tau$ on $M$ was found for PNI in 96% $H_2SO_4$ (points in Figure 9). Such a dependence observed at the relatively large $M$ values is well-known to be a reliable indication of the rigid-chain polymer molecules whose conformation changes from rod to Gaussian coil with increasing $M$. In accordance with this statement, the data points in Figure 9 agree well with curve 1, which represents the approximation developed by Tsvetkov[35] for kinetically rigid wormlike chains and given by

$$\Delta n/\Delta\tau = B\Delta\alpha M/(M + M_s) \quad (25)$$

Here $\Delta\alpha$ and $M_s$ are an optical anisotropy and mass per the Kuhn segment, respectively, and $B$ is an optical coefficient defined by

$$B = 4\pi(n_s{}^2 + 2)^2/(45k_BTn_s) \quad (26)$$

where $n_s$ is the refractive index of the solvent.

$M$ dependence of $\Delta n/\Delta\tau$ is usually characterized by the coil limit value, $(\Delta n/\Delta\tau)_\infty = \lim(\Delta n/\Delta\tau)_{M\to\infty}$ and by the initial slope, $[\partial(\Delta n/\Delta\tau)/\partial M]_{M\to 0}$. The $(\Delta n/\Delta\tau)_\infty$ value, according to eq 25, is determined by the $\Delta\alpha$ value, while the relation of $(\Delta n/\Delta\tau)_\infty$ to the initial slope is equal to $M_s$.

The best fit of experimental points in Figure 9 to a theoretical curve is achieved by

$$(\Delta n/\Delta\tau)_\infty = B\Delta\alpha = 450 \times 10^{-10}\ (\text{cm s}^2\ \text{g}^{-1}) \quad (27)$$

Hence, the best fit of Tsvetkov treatment yields

$$(\Delta n/\Delta\tau)\ (\text{cm s}^2\ \text{g}^{-1}) = 450 \times 10^{-10}M/(M + 6.7 \times 10^3) \quad (28)$$

One can see also the coil limit $(\Delta n/\Delta\tau)_\infty$ value (and, hence, $\Delta\alpha$) for PNI to be approximately 1.4 times those obtained for PABI in the same solvent (curve *2* in Figure 9). Hence, an optical anisotropy of the PNI chain segment $\Delta\alpha$ is also 1.4 times that of PABI. This exceeding is in a good agreement with higher equilibrium rigidity of the PNI chain (higher the Kuhn segment length) discussed above.

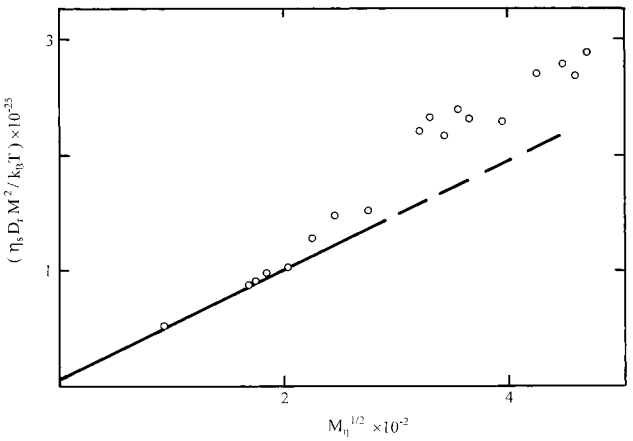


**Figure 8.** $\eta_sD_rM_\eta^2/k_BT$ *vs* $M_\eta^{1/2}$ for PNI in 96% $H_2SO_4$ (points). The solid curve represents a fit of the Hearst treatment[34] based on eq 24 for wormlike chains with $A = 160$ Å and $M_L = 25$ Da/Å.

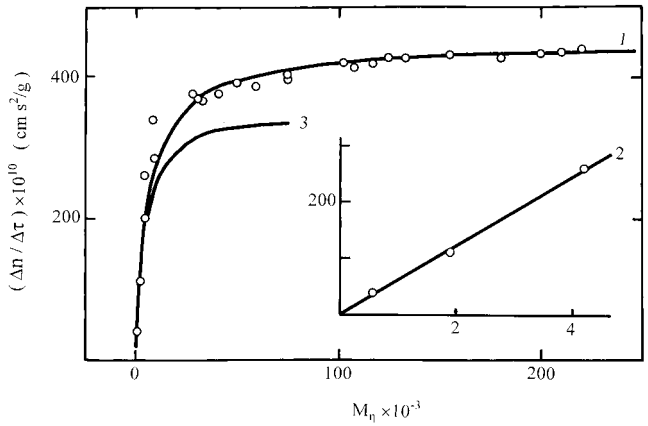


**Figure 9.** Shear optical coefficient $\Delta n/\Delta\tau$ vs molecular weight for PNI in 96% $H_2SO_4$. Solid curves represent a fit of the Tsvetkov treatment[35] based on eq 25, for the (1, 2) PNI and (3) PABI[4] molecules.

**Conformational Analysis.** The shift parameter $M_L$ was determined by use of the PNI repeat unit structure

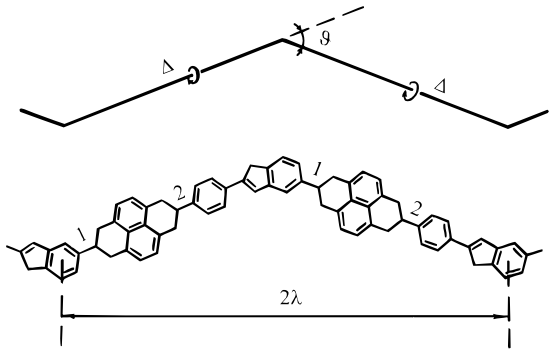


One can see that the direction of the contour chain bends at the location of the benzimidazole ring center only, and the bonds designed as 1 and 2 in the PNI structure should be considered parallel. Hence, this

molecular structure may be modeled by a chain formed with virtual bonds of rotation, with length $\Delta$ each, jointed one to another at the angle $\vartheta$. For this chain, the length per monomer unit is $\lambda = \Delta \cos(\vartheta/2)$ and $M_L = M/L = M_o/\lambda$ with $M_o$ being the mass per monomer unit.

The experimental segment length was compared with the theoretically expected one to evaluate a hindrance to the intramolecular rotations in the chain. For a freely jointed model chain shown above, a Kuhn segment length $A_{free}$ is determined by[36]

$$A_{free} = [\Delta/\cos(\vartheta/2)](1 + \cos\vartheta)/(1 - \cos\vartheta) \quad (29)$$

The application of $\Delta = 19.4$ Å and $\vartheta = 30°$ yields $A_{free} = 280$ Å. One can see that the $A_{free}$ value thus obtained greatly exceeds $A_D = 170$ Å. This result, $A_D < A_{free}$, has no physical sense at all, and indicates, most probably, that the incorrect numerical values of structure parameters $\Delta$ and $\vartheta$ were used above. We may assume that either the benzimidazole circle breaks the direction of the chain contour by an angle exceeding 30°, or coaxiality of the bonds 1 and 2 in the PNI chain structure shown above is disturbed as a consequence of the valence angle deformation. A reasonable agreement between the hydrodynamic data and a structure of the PNI chain is achieved if we assume that the $\vartheta$ angle is close to 39°, which agrees with a possible axial asymmetry of the benzimidazole circle.[37] In this case, we have $\lambda = 18.3$ Å and $M_L = 25.0$ Da/Å.

Let us now compare the $A_D$ and $A_{PABI}$ values. Coiling of the PABI chain backbone is provided by the benzimidazole ring and the amide groups. Hence, in relation to PABI, we may express the principle of the flexibilities additivity mentioned above in form

$$(\lambda/A)_{PABI} = (\lambda/A)_{PNI} + 2(\lambda/A)_{PA}$$

The numerical coefficient 2 here takes into account the number of the amide groups in the PABI monomer unit. Thus, this comparison enables one to solve the task of inversely evaluating the *p*-aromatic polyamide (PA) chain equilibrium flexibility. In fact, by setting $(\lambda/A)_{PABI} = 17.8/130$ and $(\lambda/A)_{PNI} = 18.3/170$ we obtain $(A/\lambda)_{PA} = 68$, which is close to $(A/\lambda)_{PPTA} = 400/5.2$ obtained earlier for PPTA by the same method.[2,3] To provide this result, one must take into account not only the difference between the inner angles at C and N atoms in the amide moiety ($\beta - \alpha = 7°$)[38] but also the thermal deformation (noncoplanarity) of this group ($\varphi \cong 14°$).[7,39]

**Conclusions.** Conformational analysis, establishment of the molecular-weight dependences of the hydrodynamic and optical properties, and evaluation of the equilibrium rigidity of the macromolecules of the new polyheteroarylene, PNI, were governed by the absence of noncyclic units in the polymer chain. This conclusion[10] was confirmed here by the dynamo-optical data, as a macromolecule chain irregularity due to incomplete cyclization of the monomer units results in strong structural and, hence, optical inhomogeneity of the samples that was not observed in the present work.

The translational diffusion and flow birefringence investigations were performed with the use of specially worked out devices. This permitted the determination of molecular weights of the PNI samples. The experimental fact that the hydrodynamic parameter $A_0$ remains invariable when $M$ is changing, established previously,[23] and the use of the numerical $A_0$ value correlated with the $M_{sD}$ value obtained earlier for PABI by the absolute method,[3] approaches this method of the $M$ determination by the absolute one.

With the application of new representative equations, the molecular-weight relationships of the hydrodynamic and dynamo-optical properties were established over an $M$ range from $6.7 \times 10^3$ to $2.5 \times 10^5$ (eqs 15, 18, 19, and 28). Their peculiarities show undoubtedly that PNI belongs to rigid-chain polymers. The persistense length of the PNI molecule was determined from the translational and rotational diffusion data to be $85 \pm 15$ Å. The chain diameter is close to $d = 8$ Å, and the shift factor is $M_L = 25$ Da/Å. Hence, a draining coil with Kuhn segment number from 2 to 60 is an adequate conformation of the PNI macromolecules in dilute solution for the samples investigated.

The $A$ value evaluated for the PNI molecule is high and close to that for the other rigid-chain heterocyclic polyamides.[7] However, $A$ and $\Delta\alpha$ for the PNI molecule were shown above to exceed that for PABI by approximately one-third. This seems to be reasonable if one takes into account that the combination of two amide groups and a phenyl ring in the PABI monomer unit is substituted in a PNI one by a more rigid and anisotropic naphthyleneimide cycle.

Thus, hydrodynamic and dynamo-optical data show that the structural changes (passing from PABI to PNI) by the replacement of the amide groups with a cyclic one, increase the equilibrium rigidity of the molecular chain by one-third, as a consequence of the decreasing set of physical mechanisms of the chain flexibility. Simultaneously, a comparison of the intrinsic orientation in FB (or relaxation time) with the product $M[\eta]$ shows that intramolecular motions include the large-scale deformations of the PNI chain backbone increasing with increasing $M$.

**Acknowledgment.** Authors are sincerely indebted to I. I. Ponomarev for providing the polymer samples. Careful performance of the experimental measurements by O. V. Okatova and N. P. Yevlampieva is gratefully acknowledged. The authors wish to thank one of the referees for the thorough reading of their original manuscript and for his permission to use some of his formulations in the revised text.

## References and Notes

(1) Tsvetkov, V. N.; Shtennikova, I. N. *Macromolecules* **1978**, *11*, 306.
(2) Lavrenko, P. N.; Okatova, O. V. *Polym. Sci. USSR* **1979**, *21*, 406.
(3) Vitovskaya, M. G.; Lavrenko, P. N.; Okatova, O. V.; Astapenko, E. P.; Novakovskii, V. B.; Bushin, S. V.; Tsvetkov, V. N. *Eur. Polym. J.* **1982**, *18*, 583.
(4) Shtennikova, I. N.; Peker, T. V.; Garmonova, T. I.; Mikhailova, N. A. *Eur. Polym. J.* **1984**, *20*, 1003.
(5) Lavrenko, P. N.; Strelina, I. A.; Schulz, B. *Eur. Polym. J.* **1997**, *33*, 805.
(6) Filippova, T. V.; Shtennikova, I. N.; Lavrenko, P. N. *Macromol. Chem. Phys.* **1997**, *198*, 1843.
(7) Tsvetkov, V. N. *Rigid-Chain Polymers*; Consultants Bureau: New York, 1989; pp 4, 223, 300, and 374.
(8) Shmueli, U.; Traub, W.; Rosenheck, K. *J. Polym. Sci., Polym. Phys. Ed.* **1969**, *7*, 515.
(9) Nikolskii, O. G.; Ponomarev, I. I.; Rusanov, A. L.; Vinogradova, S. V.; Levin, V. Yu. *Vysokomol. Soedin., Ser. B* **1990**, *32*, 636.
(10) Lavrenko, P. N.; Okatova, O. V.; Korshak, V. V.; Vinogradova, S. V.; Rusanov, A. L.; Ponomarev, I. I. *Polym. Sci. USSR, Ser. A* **1990**, *32*, 1139.

(11) See, for example: Roitman, D. B.; Wessling, R. A.; McAlister, J. *Macromolecules* **1993**, *26*, 5174 and references herein.
(12) Arpin, M.; Strazielle, C. *C. R. Acad. Sci., Paris* **1975**, *280*, 1293. Arpin, M.; Debeauvais, F.; Strazielle, C. *Makromol. Chem*. **1976**, *177*, 585. Arpin, M.; Strazielle, C.; Benoit, H. *Polymer* **1977**, *18*, 262. Arpin, M.; Strazielle, C. *Polymer* **1977**, *18*, 591. Milland, B.; Strazielle, C. *Makromol. Chem*. **1978**, *179*, 1261.
(13) Alfonso, G. C.; Bianchi, E.; Ciferri, A.; Russo, S.; Salaris, F.; Valenti, B. *Polym. Prepr.* (*Am. Chem. Soc., Div. Polym. Chem.)* **1977**, *18*, 179.
(14) Smirnova, V. N.; Ronova, I. A.; Prozorova, G. E.; Okromchedlidze, N. P.; Iovleva, M. M. *Vysokomol. Soed., Part B* **1987**, *29*, 710.
(15) Furukawa, R.; Berry, G. C. *Pure Appl. Chem*. **1985**, *57*, 913.
(16) Ponomarev, I. I.; Nikol'skii, O. G.; Volkova, Y. A.; Zakharov, A. V. *Polym. Sci., Ser. A* **1994**, *36*, 1185.
(17) Ponomarev, I. I.; Nikolsky, O. G. In *Polyimides and Other High-Temperature* Polymers; Abadie, M. A., Sillon, B., Eds.; Elsevier: Amsterdam, 1991; p 207.
(18) Lavrenko, P. N.; Okatova, O. V. *J. Appl. Polym. Sci*. **1995**, *56*, 97.
(19) Lavrenko, P. N.; Raglis, V. V. *Instruments Exp. Techniques* **1986**, *29*, Part 2, 496.
(20) Tsvetkov, V. N.; Andreeva, L. N. *Adv. Polym. Sci*. **1981**, *39*, 95.
(21) Lavrenko, P. N. Dr. Sci. Thesis, Institute of Macromolecular Compounds, RAS, Leningrad, 1987.
(22) Berry, G. C. *Discuss. Faraday Soc.* **1970**, *No. 49*, 121.
(23) Tsvetkov, V. N.; Lavrenko, P. N.; Bushin, S. V. *J. Polym. Sci., Polym. Chem. Ed*. **1984**, *22*, 3447.
(24) This is easily seen that $A_0$ differs from the Flory-Mandelkern invariant (Mandelkern, L.; Flory, P. J. *J. Chem. Phys*. **1952**, *20*, 212) by the multiplier $k_B$ only. The numerical coefficient 100 is introduced here for convenience in analysis of many literature data reviewed in ref 23.
(25) Kolomietz, I. P.; Tsvetkov, V. N. *Vysokomol. Soedin., Ser. B* **1983**, *25*, 813.
(26) Lavrenko, P. N. *Polymer* **1990**, *31*, 1481.
(27) Hearst, J. E.; Stockmayer, W. H. *J. Chem. Phys*. **1962**, *37*, 1425.
(28) Yamakawa, H.; Fujii, M. *Macromolecules* **1973**, *6*, 407.
(29) Yamakawa, H.; Fujii, M. *Macromolecules* **1974**, *7*, 128.
(30) See, for example: Lavrenko, P. N.; Kolomietz, I. P.; Finkelmann, H. *Macromolecules* **1993**, *26*, 6800.
(31) Bareiss, R. E. In *Polymer Handbook*; Brandrup, J., Immergut, E. H., Eds.; Wiley-Interscience: New York, 1988; part VII, p 149.
(32) Lavrenko, P. N.; Andreeva, K. A.; Strlina, I. A. *J. Thermal Anal*. **1995**, *44*, 1137.
(33) Chaeffey, C. E. *J. Chim. Phys*. **1966**, *63*, 1379.
(34) Hearst, J. E. *J. Chem. Phys*. **1963**, *38*, 1062.
(35) Tsvetkov, V. N. *Dokl. Phys. Chem*. **1982**, *266*, 786.
(36) Benoit, H. *J. Polym. Sci*. **1948**, *3*, 376.
(37) Bowen, H. J. M.; Sutton, L. E. *Tables of Interatomic Distances and Configuration in* Molecules and Ions; Royal Chemical Society: London: 1965.
(38) Erman, B.; Flory, P. J.; Hummel, J. P. *Macromolecules* **1980**, *13*, 484.
(39) Lavrenko, P. N.; Okatova, O. V. *J. Polym. Sci., Polym. Phys. Ed*. **1993**, *31*, 633.

MA980118O